Libyan Journal of Medical and Applied Sciences LJMAS
Online ISSN: 3006-1113
Volume 3, Issue 3, 2025, Page No: 81-90
Website: https://ljmas.com/index.php/journal/index

Investigation of Scattered Power and Cross-Polarization Effects on Linearly Polarized Waves under Sandstorm Conditions

Fowzi S. Alarabi [*]
Department of Networks, Faculty of Information Technology, Elmergib University, Libya.

[*]*Corresponding author: fozuy.alarbi@gmail.com*

Received: June 03, 2025 Accepted: August 17, 2025 Published: August 23, 2025

Cite this article as: F, S, Alarabi. (2025). Investigation of Scattered Power and Cross-Polarization Effects on Linearly Polarized Waves under Sandstorm Conditions. Libyan Journal of Medical and Applied Sciences (LJMAS). 2025;3(3):81-90.

Abstract:
Sand and dust storms (SDST) can significantly affect the propagation of microwave and millimeter-wave signals. These atmospheric conditions reduce visibility due to the high concentration of suspended particles, which enhances the scattering of electromagnetic waves. The extent of signal power loss and distortion depends on particle characteristics, such as size, shape, and orientation, as well as wave polarization and incidence angle.
In this work, the modified Rayleigh approximation is employed to estimate the scattered power and the cross-polarization generated by sand and dust particles. This formulation enables accurate characterization of the scattering behavior of non-spherical particles with triaxial ellipsoidal geometry in the microwave and millimeter-wave frequency ranges. The results reveal a clear dependence of the scattered power distribution between horizontal and vertical polarization components on particle geometry, with the effect being more pronounced in the case of horizontally aligned particles, a configuration considered physically realistic due to gravitational settling and the influence of horizontal wind shear.
Scattered power in the microwave and millimeter-wave bands is further formulated as a function of meteorological visibility by establishing a relationship between sand/dust particle concentration and visibility range. The results demonstrate that scattering effects intensify considerably with the severity of SDST, as indicated by reduced visibility. In this study, cross-polarization discrimination (XPD) is evaluated as the ratio between the received co-polarized power and the corresponding power in the orthogonal component, in order to quantify the transfer of energy into the cross-polarized state induced by dust particles. Such studies are essential for the design of terrestrial wireless communication systems in desert environments, particularly polarization-sensitive links operating at high frequencies (40–80) GHz).

Keywords: Polarizability, Scattering Cross Section, Electromagnetic Scattering, Modified Rayleigh Approximation, Ellipsoidal Shape.

دراسة تأثيرات القدرة المتبعثرة والاستقطاب المتقاطع على الموجات ذات الاستقطاب الخطي في ظل ظروف العواصف الرملية

فوزي الصادق العربي [*]
[1] قسم الشبكات، كلية تقنية المعلومات، جامعة المرقب، ليبيا

الملخص
يمكن أن تؤثر العواصف الرملية والترابية (SDST) بشكل كبير على انتشار إشارات الموجات الميكروية والملي مترية. تؤدي هذه الظروف الجوية إلى انخفاض مدى الرؤية نتيجة الارتفاع الكبير في تركيز الجسيمات العالقة، مما يعزز من عملية تشتت الموجات الكهرومغناطيسية. ويعتمد مقدار الفقد في قدرة الإشارة والتشوه الناتج عنها على خصائص الجسيمات مثل الحجم والشكل والاتجاه، بالإضافة إلى استقطاب الموجة وزاوية السقوط.

في هذا العمل، تم استخدام تقريب ريلي المعدل لتقدير القدرة المتبعثرة والقدرة المتولدة في الاستقطاب المتقاطع بفعل جسيمات الرمل والغبار. وتتيح هذه الصياغة توصيفًا دقيقًا لسلوك التبعثر للجسيمات غير الكروية ذات الشكل الإهليجي ثلاثي المحاور ضمن نطاقات التردد الخاصة بالموجات الميكروية والملي مترية. وقد أظهرت النتائج اعتمادًا واضحًا لتوزيع القدرة المتبعثرة بين مكونات الاستقطاب الأفقي والعمودي على شكل الجسيمات،

حيث كان هذا التأثير أكثر وضوحًا في حالة محاذاة الجسيمات أفقيًا، وهو تكوين يُعتبر واقعيًا من الناحية الفيزيائية نتيجة الترسيب بالجاذبية وتأثير القص الهوائي الأفقي.

كما تمت صياغة القدرة المتبعثرة في نطاقي الموجات الميكروية والملي مترية كدالة في الرؤية الجوية من خلال الربط بين تركيز جسيمات الرمل/الغبار ومدى الرؤية. وأوضحت النتائج أن تأثيرات التبعثر تزداد بشكل ملحوظ مع اشتداد العواصف الرملية والترابية، كما يتضح من الانخفاض الكبير في مدى الرؤية. في هذه الدراسة، تم تقييم (XPD)كنسبة بين القدرة المستقبلة في الاستقطاب الأصلي (Co-Pol) والقدرة المناظرة في المكون المتعامد، وذلك من أجل توصيف انتقال القدرة إلى حالة الاستقطاب المتقاطع بفعل جسيمات الغبار. وتُعد مثل هذه الدراسات ضرورية لتصميم أنظمة الاتصالات اللاسلكية الأرضية في البيئات الصحراوية، خصوصًا الروابط الحساسة للاستقطاب التي تعمل عند الترددات العالية (40–80).

الكلمات المفتاحية: القابلية للاستقطاب، المقطع العرضي للتبعثر، التبعثر الكهرومغناطيسي، تقريب ريلي المعدل، الشكل الإهليلجي.

Introduction

The propagation of microwave and millimeter-wave signals in desert environments is significantly affected by Sand and dust storm (SDST). These weather conditions degrade signal quality through both scattering and absorption caused by suspended particles in the atmosphere. As visibility decreases during such events, the particle number density increases, thereby intensifying these propagation impairments. Microwave and millimeter-wave links, commonly used in terrestrial and satellite communication systems, are particularly susceptible to attenuation and depolarization effects. These impairments reduce signal strength and distort polarization states, leading to increased cross-polarization interference, reduced link margins, and lower communication reliability.

This work investigates these effects by applying the modified Rayleigh approximation scattering theory to model signal interactions with non-spherical, horizontally aligned dust particles.

The effect of dust particles on the transmitted power of linearly polarized signals was studied, and the amount of power scattered in the cross direction was estimated for each linear polarization case. The amount of cross-polarization was also calculated as a ratio of the transmitted signal to the scattered signal, and these relationships were related to frequency and range of vision. This paper also included the effect of the angle of incidence of the linearly polarized wave on dust particles and an estimation of the amount of scattered power.

SDST affect vast areas of land across Libya. Dust particles generated during such events degrade the quality of communication links by attenuating signals along the propagation path. Several Libyan researchers [4],[19],[20], and [21] have examined the impact of sand and dust storms on the performance of microwave links, particularly by calculating the complex permittivity of sand and dust particles and estimating particle density, both of which are applied in the present work.

Although many previous studies in this field [7], and [19] have focused on attenuation caused by spherical sand / dust particles, they have often neglected the effects of non-spherical particle shapes on scattered power and cross-polarization discrimination (XPD). Therefore, this study investigates a monodisperse medium composed of non-spherical dust particles using the modified Rayleigh scattering approach, which is applicable in both microwave and millimeter-wave bands.

To illustrate the scattering effects in microwave and millimeter-wave links under sand and dust storm conditions, this work also introduces expressions that relate storm severity (represented by visibility) to the particle concentration. This quantity is often difficult to quantify directly. These expressions contribute to estimating the scattered power in the cross-polarization component of linearly polarized waves**.**

Modified Rayleigh Approach and Particle Geometry

Modified Rayleigh Approximation (MRA).

The Modified Rayleigh Approximation (MRA) is an extension of the classical Rayleigh scattering theory, developed to overcome the limitations of the original formulation in modeling non-spherical particles and materials with more complex properties. While the classical Rayleigh theory applies only to electrically small, homogeneous, isotropic, and perfectly spherical particles, the MRA offers a more general framework that accommodates anisotropic, ellipsoidal particles (e.g., spheroidal or triaxial shapes). The modified Rayleigh approach can be formulated under the assumptions that the particle is placed in a uniform, homogeneous electric field [2] and that its radius is much smaller compared to the wavelength, as follows:

$$y = \mathrm{k.a} < 1 \qquad (1)$$

Where

k = a propagation constant $= \frac{2\pi}{\lambda}$.

λ = the transmitting wavelength.

a = the radius of the dust particle.

The second assumption concerns the contrast in refractive index *m* between the particle and the surrounding medium. The product of the size parameter and the complex refractive index magnitude must remain below unity $\boldsymbol{k|m|a < 1}$ to limit phase distortion and ensure the quasi-static approximation remains valid.

The third assumption involves the dielectric constant ε. The condition.

$$\mathrm{k\,.\,a.}\,|\varepsilon - 1| \ll 1 \qquad 2$$

Must be fulfilled to prevent excessive polarization inside the particle and to maintain the validity of the dipole approximation. When these conditions are jointly satisfied, the MRA provides accurate estimates of scattering and depolarization behaviors for particles within the microwave and millimeter-wave frequency ranges.
Typically, MRA remains valid for y $\lesssim$ 0.3 - 0.5 [5], depending on the particle shape and complex permittivity. This condition ensures that the particle is much smaller than the incident wavelength.
To establish a practical interpretation of the "much less than 1" condition in Eq. (2), a threshold of 0.5 is adopted as the reference limit. In this study, the relevant assumptions and conditions were evaluated for applicability. For instance, at 100 GHz, the computed values of the wave number ka and the size parameter $k|m|$a are approximately 0.25 and 0.45, respectively, based on a dielectric constant of ε = 6.089 – j0.165 for dry dust particles as reported in the literature [4]. The third condition applies to the millimeter wavelength range, with frequencies less than 80 GHz
Since the primary criterion is size relative to wavelength, MRA is typically applicable in the microwaves and millimeter waves, depending on the actual particle size.

Particle Geometry and Depolarization Factors.
Non-spherical dust particles are represented using triaxial ellipsoids defined by semi-axes (a_1, a_2, a_3), adopting axis ratios of 1:0.71:0.53 [8]. This specific configuration captures the elongated and compressed geometry commonly observed in natural dust and sand particles [7]. Utilizing a triaxial ellipsoidal model enables a more precise estimation of scattering and depolarization phenomena compared to traditional spherical representations.
Assuming the particles are elongated and horizontally aligned, the Depolarization Factors are geometric coefficients that determine how an external electric field induces dipoles inside the ellipsoidal particle along each axis. For each principal axis $i \in \{1, 2, 3\}$, the depolarization factor Li is computed using the following integral [9][10]:

$$L_i = \frac{1}{2}\int_0^{\infty} \frac{a_1 a_2 a_3}{(s + a_i^2)\sqrt{(s + a_1^2)(s + a_2^2)(s + a_3^2)}}\, ds \qquad 3$$

This integral is evaluated numerically using Gaussian quadrature. In the Python-based implementation employed in this work, the scipy.integrate.quad function is utilized with a sufficiently large upper limit to approximate an infinite bound.
Given the axis ratios used, the depolarization factors L_1, L_2, and L_3 can be associated with the major, intermediate, and minor axes, respectively. Under this configuration, L_1, corresponds to the horizontal axis, while L_2 and L_3 lie along the vertical orientation [9].
These values serve as fundamental inputs for computing the polarizability of the particle along different directions, which directly influences the backscattering strength in both horizontal and vertical polarizations. They are subsequently used to calculate the scattering cross-sections and the power scattered in the cross-polarized component.

Dust Concentration and Visual Range
The scattering calculations of the wave along the propagation path during SDST depend on the particle radius, the wavelength, and the particle number density. However, the particle number density (per unit volume) is a parameter that is difficult to measure in SDST. Therefore, efforts are made to relate particle concentration to visibility, as SDST are typically identified and monitored meteorologically based on visibility. Accordingly, in this study, the evaluation of scattering is further addressed in terms of visibility.
An empirical relationship between dust concentration and visibility has been proposed in [7], [8], and [12]. These formulations allow for practical application across various SDST conditions. They also offer a means of estimating dust particle concentrations based on observed visibility levels. Such expressions have been widely adopted by researchers in the field.
The particle density or volume fraction can be expressed as a function of visibility, based on the relationship described in [12],[13] as follows:

$$\nu = \frac{c}{\rho_0 \cdot V^{\gamma}} \qquad 4$$

Where
ρ_0= the solid density of dust $kg/m3$
ν = the relative volume or volume fraction.

V = the visibility (km)
C and γ constants dependent on climatic conditions and origin of the storms, to be 2.3×10^{-5} and 1.07 respectively [7].
If Eq. (4) is divided by the solid density of dust (ρ_0 = 2327 kg/m³), as obtained in [4], Eq. (5) is derived.

$$\nu = \frac{9.88 \times 10^{-9}}{V^{\gamma}} \qquad 5$$

For particles modeled as ellipsoids with three unequal axes, the physical volume V_P of the particle is given by the following equation:

$$V_P = \frac{4}{3}\pi a_1 a_2 a_3 \qquad 6$$

The volume fraction associated with N equivalent dust particle scatterers can be defined as:

$$\nu = V_P * N \qquad 7$$

Combining (4) and (5) yields the following expression:

$$N = \frac{2.369 \times 10^{-9}}{V^{\gamma} a_1 a_2 a_3} \qquad 8$$

The dust particle concentration was estimated based on an assumed equivalent particle radius of a =75 μm.

Polarization and Scattering Analysis

When electromagnetic waves interact with suspended atmospheric particles (such as dust or sand), changes in polarization occur as a result of scattering [14].

Scattering refers to the redirection of electromagnetic energy by particles, and its strength depends on particle shape, size, material properties, and alignment. Polarization describes the orientation of the electric field vector of the wave. In dusty environments, the interaction between polarized waves and non-spherical particles leads to depolarization, i.e., energy transfer from one polarization state to another. This is crucial in determining the cross-polarized components of the wave, which affect the signal's quality.

This section introduces the modeling of polarizability, scattering cross-section, and scattered power to evaluate the impact of sand and dust particles on microwave propagation.

Polarizability

Polarizability α depends on the particle size, the dielectric constant, and the depolarization factors determined by the particle's shape. It is computed along one of the axes (i = 1, 2, 3) as follows: [15]

$$\alpha_i = V * \varphi_i \qquad 9$$

Where

$$\varphi_i = \frac{\varepsilon_r - 1}{1 + L_i(\varepsilon_r - 1)} \quad = \quad \acute{\varphi}_i - j\,\ddot{\varphi}_i \qquad 10$$

From (10), and assuming the three depolarization vectors l_1, l_2, and l_3. Eq. (9) may be expressed as:

$$\alpha_H = V_P\,(\acute{\varphi}_1 - j\,\ddot{\varphi}_1 \;+\; \acute{\varphi}_2 - j\,\ddot{\varphi}_2\;) \qquad 11$$

$$\alpha_V = V_p\;(\acute{\varphi}_i - j\,\ddot{\varphi}_i\;) \qquad 12$$

Where α_H and α_V are the Polarizability of particles along horizontal and vertical axis, respectively.

Scattering Cross Section According to the modified Rayleigh scattering theory, the scattering cross-section (σ), which quantifies the power scattered by an individual particle, is given in [19].

$$\sigma_{sc}^{j} = \frac{8\pi^3}{3\lambda^4}|\alpha_i|^2 \qquad j = \mathrm{h, v} \qquad 13$$

In the study of electromagnetic scattering by small particles, understanding the angular distribution of the scattered field's polarization is essential for characterizing depolarization effects. Cross-polarization occurs when the scattered field contains a component that is orthogonal to the polarization of the incident wave. In Rayleigh scattering, such effects are especially pronounced for non-spherical particles [9].

Assuming that the incident electromagnetic wave is linearly polarized along the y-axis and propagates in the z-direction, the scattered field can be analyzed to isolate the cross-polarized component. This is achieved by projecting the scattered electric field onto a unit vector $\hat{e}_{cross}$, which is orthogonal to both the incident electric field vector $\vec{E}_{inc}$ and the scattering plane. The differential scattering cross-section for this component is given by [23]:

$$\frac{\partial\sigma}{\partial\Omega_{cross}} = \frac{8\pi^3}{3\lambda^4}.|\alpha_i|^2.\;\left|\hat{e}_{cross}\left(\hat{r}\;.\;(\hat{r}.\hat{e}_{inc})\right)\right|^2 \qquad 14$$

Where

$\hat{e}_{inc=}\,\hat{y}$

r = The unit observation vector in spherical coordinates and is given by [24]:

$$\hat{r} = \sin\theta\cos\phi\,\hat{x} + \sin\theta\sin\phi\,\hat{y} + \cos\theta\,\hat{z} \quad (15)$$

the observation direction is selected to lie in the x-y plane, corresponding to a scattering angle $\theta = 90$ and an azimuthal angle $\phi = 45$, a configuration in which the cross-polarized component is expected to be maximized. Under these conditions, $\hat{e}_{cross} = \frac{1}{\sqrt{2}}(\hat{x} - \hat{y})$, and $\hat{r} = \frac{1}{\sqrt{2}}(\hat{x} + \hat{y})$, Substituting these expressions into Eq. (15), yields the following form:

$$\frac{\partial\sigma}{\partial\Omega_{cross}} = \frac{2\pi^3}{3\,\lambda^4}|\alpha_i|^2 \quad (16)$$

Scattered Power

Assuming a uniform incident plane wave of power density S, and using respective scattering cross section the total power scattered by an individual particle is given by [9],[23]:

$P_{sc}^{j} = \mathrm{S}.\,\sigma_{sc}^{j}$ (17)

Where

S =Incident power density (W/m²) $= \frac{p_s}{4\pi r^2}$

p_s = Transmitted power (assumed 100 watts)

r = **radial distance from the antenna**(m)

The scattered power can be calculated based on the particle concentration, which is related to the visibility along the propagation path *D* through the following relation:

$P_{sc}^{j} = \mathrm{S}.\,\sigma_{sc}^{j}.\mathrm{N}\,.D$ (18)

Similarly, the cross-polarized scattered power can be computed using the effective differential scattering cross-section, which is derived from Eq. (16).

Cross Polarization Discrimination (XPD)

In linearly polarized wireless communication systems, maintaining polarization purity is essential for ensuring signal integrity and minimizing interference between orthogonal channels. One key parameter used to evaluate the impact of polarization distortion is the XPD, which quantifies the ratio of the power received in the intended polarization to that in the orthogonal (cross-polarized) component [11].

The XPD can be calculated using the following expression [25][6].

$$\mathrm{XPD(dB)} = 10\,log_{10}\left(\frac{p_{\mathrm{co-pol}}}{p_{\mathrm{cross-pol}}}\right) \quad (19)$$

Where

$P_{\text{co-pol}}$: is the received or transmitted power in the co-polarized component (i.e., same as transmitted polarization p_h or p_v).

$P_{\text{cross-pol}}$: is the power scattered into the cross-polarized component due to interaction with dust particles.

Results and Discussion

The results obtained from simulations performed using Python and its associated libraries provide valuable insights into the behavior of microwave and millimeter-wave signals under sandstorm conditions**.** Specifically, we analyze the scattered power for both horizontal and vertical polarizations as well as the resulting XPD, across a wide range of visibility conditions, from 1 meter to 300 meters.

The numerical results of the scattered power for both horizontal and vertical polarizations, obtained through Python-based simulations and presented in Figures 1–4, demonstrate a clear increasing trend as visibility decreases. This behavior is consistent with physical expectations, since higher dust concentrations corresponding to lower visibility induce stronger scattering, thereby diminishing the received power while simultaneously enhancing the scattered power.

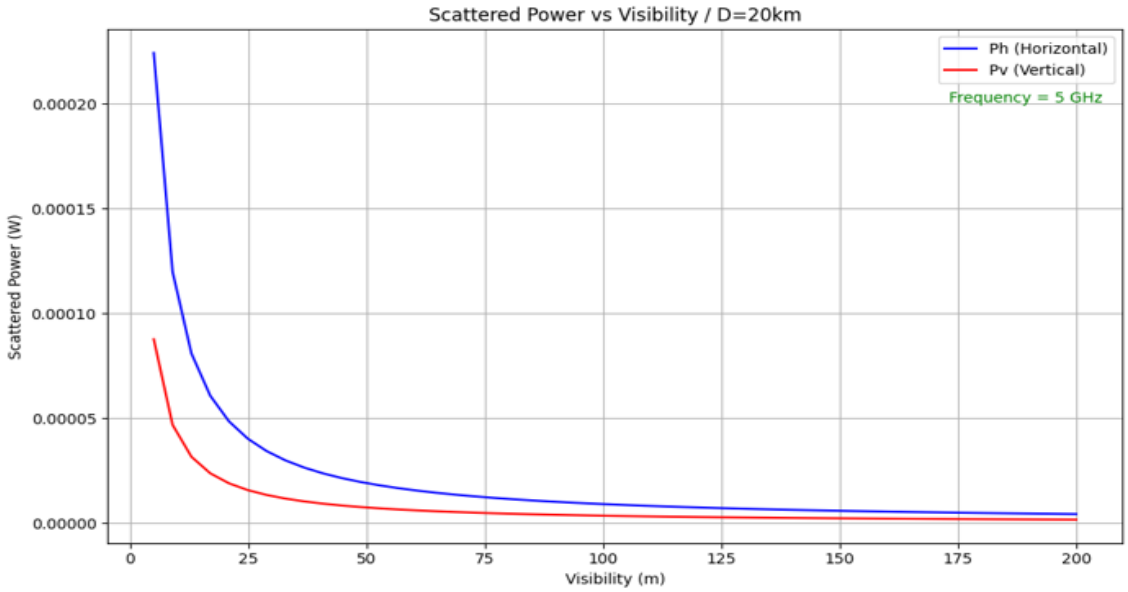

Figure1. Scattered Power against visibility at 5GHz and 20km.

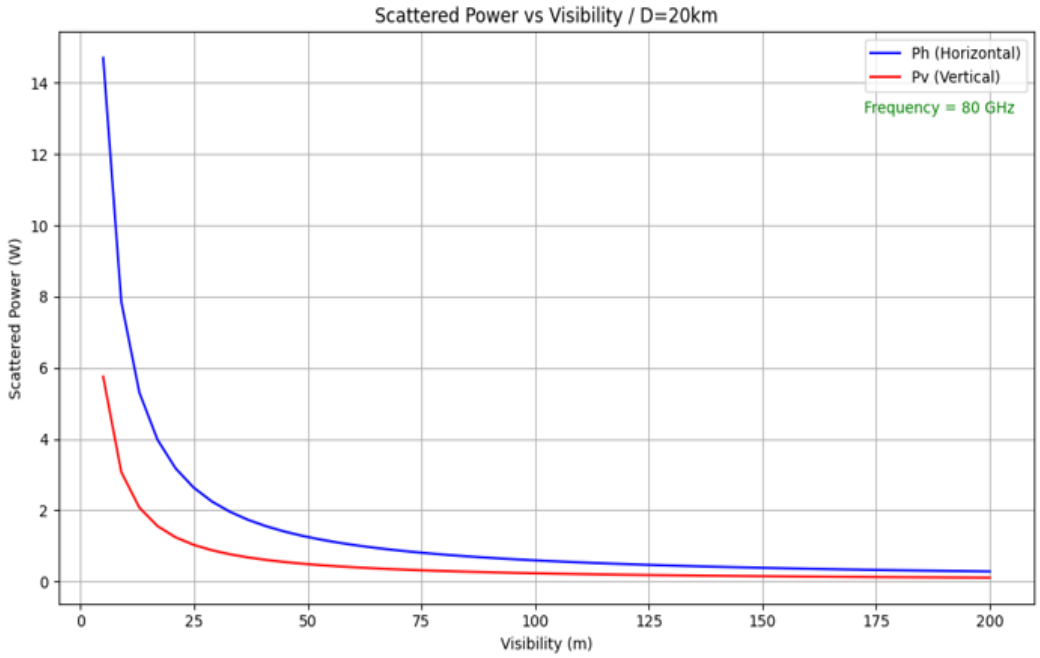

Figure2. Scattered Power against visibility at 20GHz and 20km.\

At very low visibility levels (Less than 25 meters), the difference between Scattered power in horizontal and vertical polarization becomes noticeable, reflecting the anisotropic nature of ellipsoidal particles, which interact differently with horizontally and vertically polarized waves due to their shape.

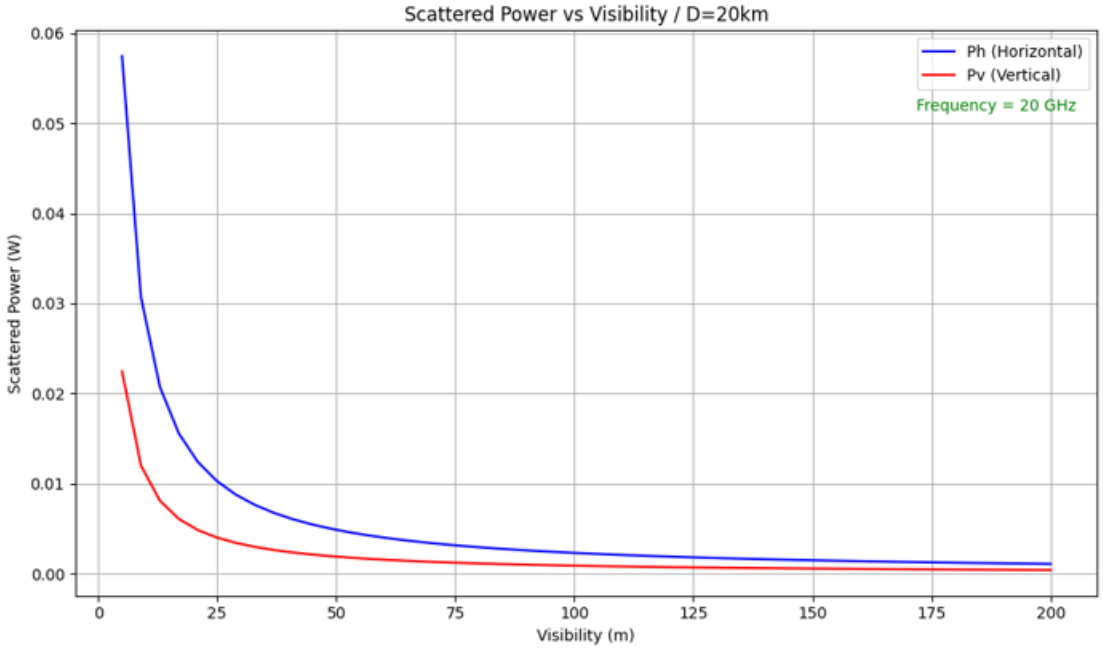

Figure3. Scattered Power against visibility at 40GHz and 20km.

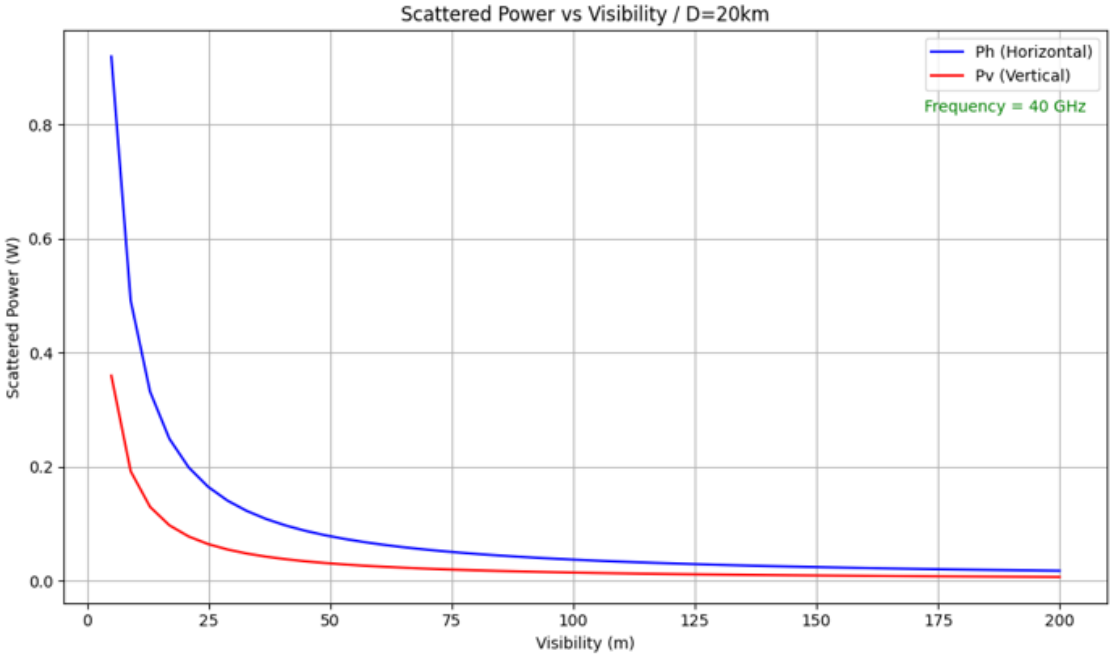

Figure4. Scattered Power against visibility at 80GHz and 20km.

Figures 5–7 illustrate the computed values of XPD, defined as the ratio of the transmitted power to the power scattered into the orthogonal polarization. The results reveal a pronounced decrease in XPD under very low visibility conditions, indicating strong wave depolarization. This behavior is attributed to the enhanced interaction between the wave and the increased number of particles, which leads to greater leakage of energy from the co-polarized component into the cross-polarized component.

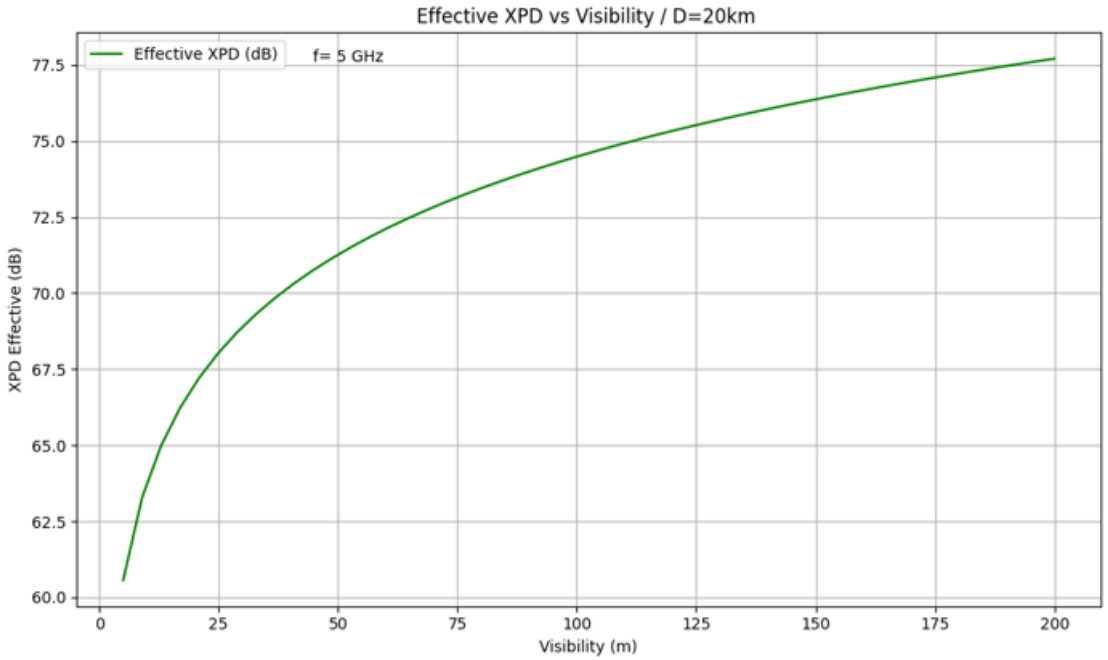

Figure5. XPD against visibility at 5GHz and 20km.

At higher visibilities (e.g., >150 m), XPD improves, indicating weaker depolarization and more reliable transmission for polarization-sensitive systems.

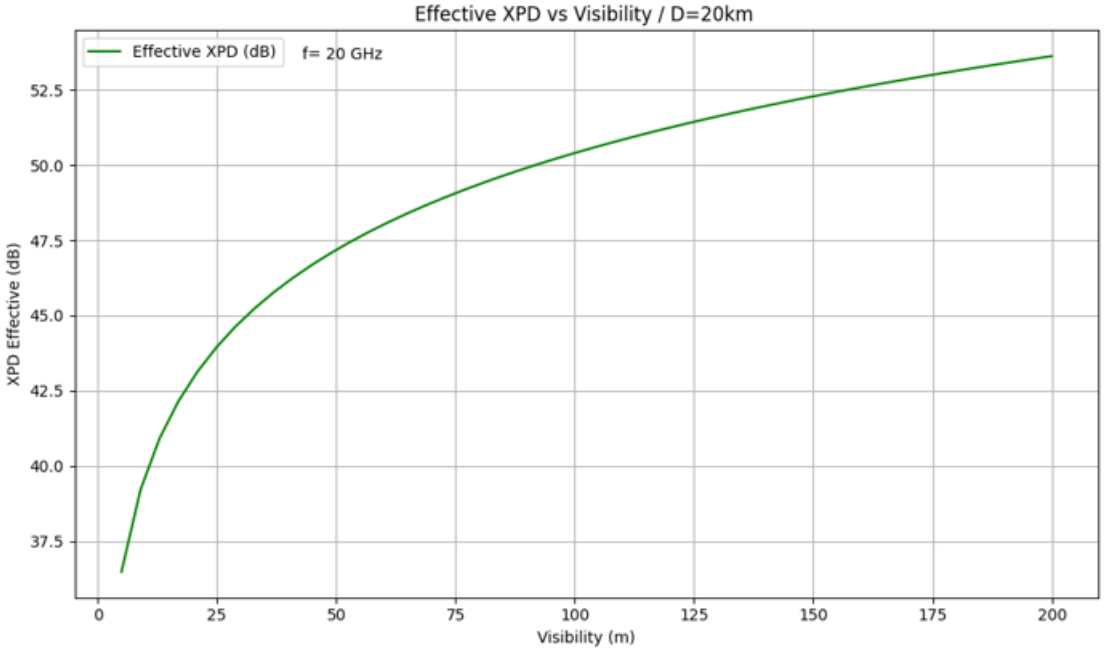

Figure6. XPD against visibility at 20GHz and 20km.

The adoption of triaxial ellipsoid geometry enables a more accurate representation of the scattering behavior, which would otherwise be underestimated if spherical models were applied. These findings are particularly relevant to linearly polarized wave systems operating in the microwave and millimeter-wave bands, such as 5G backhaul links and satellite communications, where polarization effects play a critical role in system performance. The results presented in this paper can be utilized to predict the total scattered power as well as the power coupled into the cross-polarized component due to sand and dust particles under varying visibility conditions in desert environments. For microwave systems operating in arid regions, the adoption of cross-polarization diversity techniques or adaptive modulation schemes is recommended to mitigate performance degradation during sandstorms.

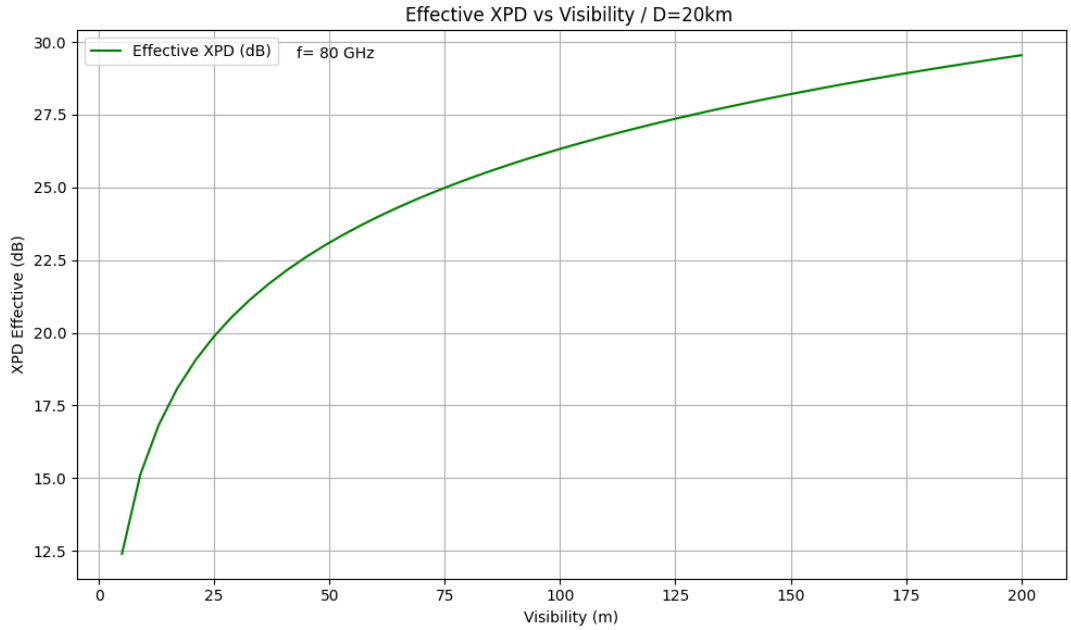

Figure7. XPD against visibility at 80GHz and 20km.

Conclusion

In this paper, the scattering of linearly polarized transmitted signals in the microwave and millimeter-wave frequency bands was investigated, considering anisotropic scattering influenced by the shape, orientation, and alignment of sand and dust particles. Non-spherical particles were modeled as triaxial ellipsoids, and the results showed that the scattered power in both polarization components increases significantly under low-visibility conditions, with this effect becoming more pronounced at higher frequencies, thereby exacerbating the vulnerability of millimeter-wave systems.

Additionally, the cross-polarization discrimination (XPD) was analyzed by estimating the power scattered into the orthogonal polarization of a horizontally polarized transmitted wave. A specific observation direction was selected to determine the scattering and azimuth angles, ensuring that the scattering was evaluated in the direction orthogonal to the transmitted polarization.

The modified Rayleigh scattering model for ellipsoidal particles with polarizability was employed to estimate both the scattered power and cross-polarization as a function of visibility. Future work may include modeling random particle orientations, Mie scattering for larger particles, and experimental validation under real field conditions.

References

1. Tsang, L., Kong, J. A., Ding, K. H., & Ao, C. O. (2004). Scattering of electromagnetic waves: numerical simulations. John Wiley & Sons.
2. Bashir, S. O. (2008, November). Electromagnetic scattering computation methods for very small particles: Part II. In Proc. of Int. Conf. Modelling & Simulation (pp. 18-20).
3. Ahmed, A. S. (1987, February). Role of particle-size distributions on millimetre-wave propagation in sand/dust storms. In IEE Proceedings H (Microwaves, Antennas and Propagation) (Vol. 134, No. 1, pp. 55-59). IEE.
4. Alarabi, F. (2022). Sand Particle-Size Distribution in Air and their Effect on Microwave Propagation: Sand Particle-Size Distribution in Air and their Effect on Microwave Propagation. Elmergib Journal Of Electrical and Electronic Engineering ISSN: 2959-0450, 1(1), 24-34.
5. Gong, S., Huang, J., & Zhao, X. (2008). Rain-induced effects on the envelope probability density functions in multipath channels. Radio science, 43(02), 1-11.
6. Xing, Y., Kanhere, O., Ju, S., Rappaport, T. S., & MacCartney, G. R. (2018, August). Verification and calibration of antenna cross-polarization discrimination and penetration loss for millimeter wave communications. In 2018 IEEE 88th Vehicular Technology Conference (VTC-Fall) (pp. 1-6). IEEE.
7. Ghobrial, S. A. M. I. R. I., & Sharief, S. A. M. I. M. (1987). Microwave attenuation and cross polarization in dust storms. IEEE transactions on antennas and propagation, 35(4), 418-425.
8. Musa, A., Bashir, S. O., & Abdalla, A. H. (2014). Review and assessment of electromagnetic wave propagation in sand and dust storms at microwave and millimeter wave bands---Part I. Progress In Electromagnetics Research M, 40, 91-100.

9. Bohren, C. F., & Huffman, D. R. (2008). Absorption and scattering of light by small particles. John Wiley & Sons.
10. Sihvola, A., & Lindell, I. V. (1990). Polarizability and effective permittivity of layered and continuously inhomogeneous dielectric ellipsoids. Journal of Electromagnetic Waves and Applications, 4(1), 1-26.
11. Alejos, A. V., Garcia Sanchez, M., & Cuinas, I. (2012). Performance analysis of polarization diversity for indoor scenarios at 41.4 GHz and 61.5 GHz. International Journal of Antennas and Propagation, 2012(1), 681820.
12. Liu, J. K., Liu, D., & Alsdorf, D. (2014). Extracting ground-level DEM from SRTM DEM in forest environments based on mathematical morphology. IEEE Transactions on Geoscience and Remote Sensing, 52(10), 6333-6340.
13. Al-Dousari, A. M., Al-Awadhi, J., & Ahmed, M. (2013). Dust fallout characteristics within global dust storm major trajectories. Arabian Journal of Geosciences, 6(10), 3877-3884.
14. Mukai, S., Hioki, S., & Nakata, M. (2023). Biomass burning plume from simultaneous observations of polarization and radiance at different viewing directions with SGLI. Remote Sensing, 15(22), 5405.
15. Li, A. (2008). Optical properties of dust. In Small bodies in planetary systems (pp. 1-22). Berlin, Heidelberg: Springer Berlin Heidelberg.
16. Hogan, R. J., Honeyager, R., Tyynelä, J., & Kneifel, S. (2017). Calculating the millimetre-wave scattering phase function of snowflakes using the self-similar Rayleigh–Gans Approximation. Quarterly Journal of the Royal Meteorological Society, 143(703), 834-844.
17. Westbrook, C. D. (2014). Rayleigh scattering by hexagonal ice crystals and the interpretation of dual-polarisation radar measurements. Quarterly Journal of the Royal Meteorological Society, 140(683), 2090-2096.
18. Min, M., Hovenier, J. W., & de Koter, A. (2003). Shape effects in scattering and absorption by randomly oriented particles small compared to the wavelength. Astronomy & Astrophysics, 404(1), 35-46.
19. Lu, Y., Clothiaux, E. E., Aydin, K., & Verlinde, J. (2014). Estimating ice particle scattering properties using a modified Rayleigh-Gans approximation. Journal of Geophysical Research: Atmospheres, 119(17), 10471-10484.
20. Abuhdima, E. M., & Saleh, I. M. (2010, April). Effect of sand and dust storms on microwave propagation signals in southern Libya. In Melecon 2010-2010 15th IEEE Mediterranean Electrotechnical Conference (pp. 695-698). IEEE.
21. Alarabi, F. S. (2023). Phase Difference between Horizontally and Vertically Polarized Microwave Signals During Sand Storms. 208-216 ,(14) ,مجلة البيان العلمية.
22. Budalal, A. A., Sharif, K. I., Hewadia, S. G., & Budalal, R. A. (2023, September). Performance Evaluation of Satellite Communication Link at Millimeter Wave Based on Rain Fade Data Measured in Libya. In International Conference for Information and Communication Technologies (pp. 55-67). Cham: Springer Nature Switzerland.
23. Mishchenko, M. I., Travis, L. D., & Lacis, A. A. (2002). Scattering, absorption, and emission of light by small particles. Cambridge university press.
24. Balanis, C. A. (2016). Antenna theory: analysis and design. John wiley & sons.
25. Challita, F., Laly, P., Liénard, M., Tanghe, E., Joseph, W., & Gaillot, D. P. (2019). Hybrid virtual polarimetric massive MIMO measurements at 1.35 GHz. IET Microwaves, Antennas & Propagation, 13(15), 2610-2618.